Supporting Information

Impacts of backwashing on micropollutant removal and associated microbial assembly processes in sand filters

Donglin Wang[1,2,★], Jie Zhou[1,2,★], Hui Lin[1,2], Junwen Chen[3], Jing Qi[1], Yaohui Bai[1,*], Jiuhui Qu[1,3]

[1] Key Laboratory of Drinking Water Science and Technology, Research Center for Eco-Environmental Sciences, Chinese Academy of Sciences, Beijing 100085, China

[2] University of Chinese Academy of Sciences, Beijing 100049, China

[3] Center for Water and Ecology, State Key Joint Laboratory of Environment Simulation and Pollution Control, School of Environment, Tsinghua University, Beijing 100084, China

* Corresponding author. E-mail address: yhbai@rcees.ac.cn (Yaohui Bai)

★ These authors contributed equally to this work.

S1: SUPPLEMENTARY METHODS

DNA extraction and 16S rRNA sequencing

Approximately 0.5 g of biofilmed sand in the surface (~1 cm) of filters was used for DNA extraction using a DNeasy Power Soil Isolation Kit (QIAGEN, Germany) according to the manufacturer's recommendations. A total of 104 DNA samples were then sent to the Beijing Genomics Institute (BGI, China) for 16S rRNA sequencing using the V4-specific primer pair 515F/806R with an amplicon size of 250 to 300 bp. The 16S rRNA sequences were analyzed using the QIIME2 pipeline (v2019.4)(Bolyen et al., 2019) to infer amplicon sequence variants (ASVs). The taxonomy of the representative sequences was classified with the RDP classifier. Based on the ASVs obtained, we then calculated the beta diversities.

Statistical analysis

All analyses were conducted in the R Environment (v 3.6.2). For beta-diversity analyses, we used phyloseq to calculate Bray-Curtis distance on ASV counts normalized via variance-stabilizing transformation. We carried out unconstrained principal coordinate analysis using the pcoa() function. All plots were generated with ggplot2.

Dissimilarity and correlation analysis of microbial community

A comparison of community dissimilarity between before and every time point after backwashing was performed by calculating Bray-Curtis distances with adonis() function in the vegan package. The Pearson correlation coefficient was calculated by a

cor() function using the mean of 3 replicates from each condition at each time point and visualized by using the corrplot package.

Differential abundance testing

The DESeq2 package was used to implement negative binomial generalized models to test the effect of experimental factors on the abundance of individual ASVs. The models set collection time point as fixed effects. Within each time point after backwashing, Wald tests were performed to compare every time point (0h, 6h, 12h, 24h and 48h) against before backwashing. For each contrast, effect size shrinkage was performed using the lfcShrink() function to rank ASVs by effect size and for visualization. To account for multiple tests within and across contrasts, all comparisons performed within two types of filter sands were pooled together before using false discovery rate (FDR, Benjamini–Hochberg procedure) to adjust P values. Groups of differentially abundant ASVs with similar responses were identified by performing hierarchical clustering (Ward's algorithm) on shrunken log fold changes with the hclust() function, details of the cluster numbers displayed in Figures S2 and S4.

S2: SUPPLEMENTARY FIGURES

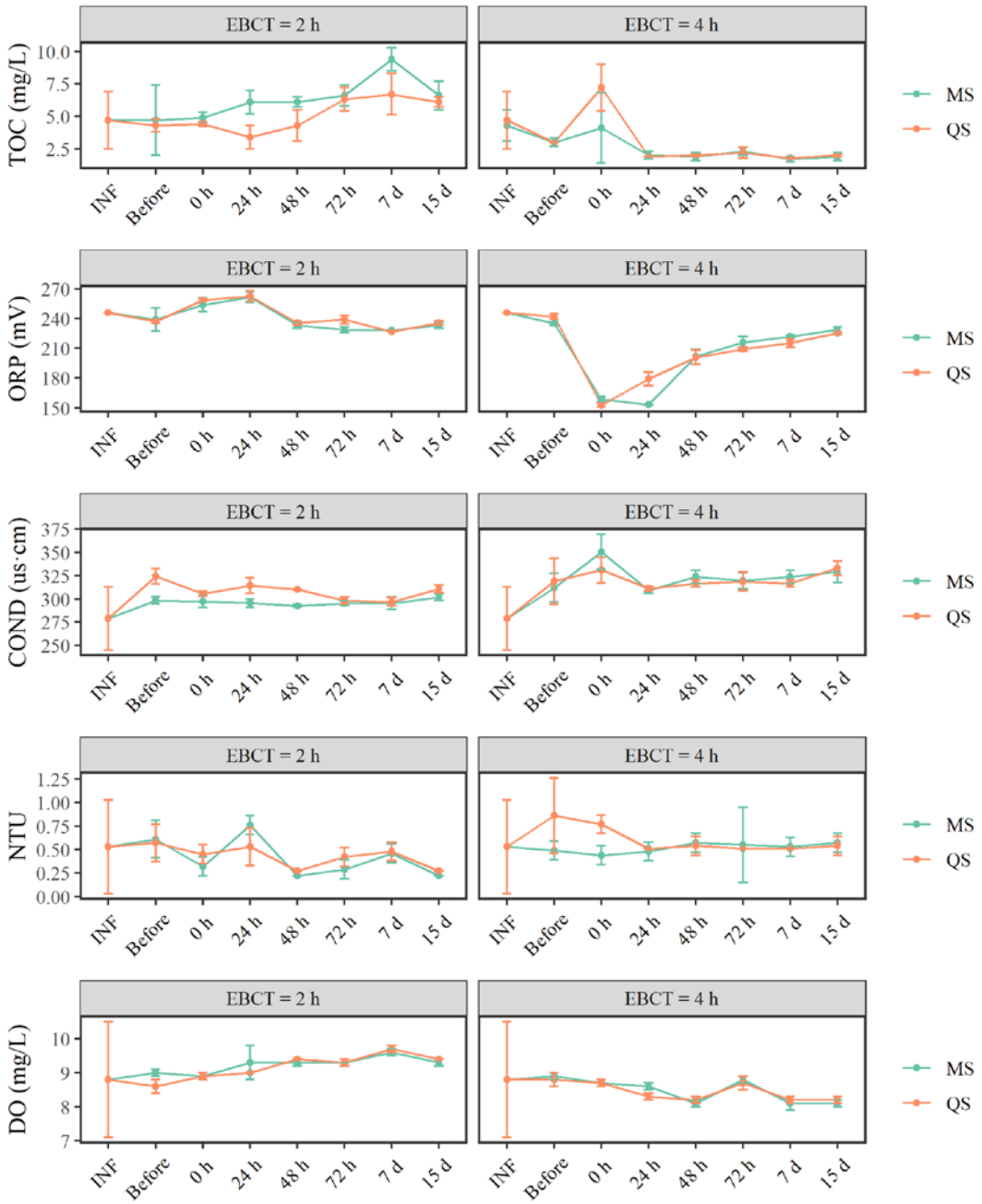

Figure S1. Variations in concentrations of total organic carbon (TOC), oxidation-reduction potential (ORP), conductivity (COND), turbidity (NTU), and dissolved oxygen (DO) in two types of sand filters. MS, manganese sand filter; QS, quartz sand filter.

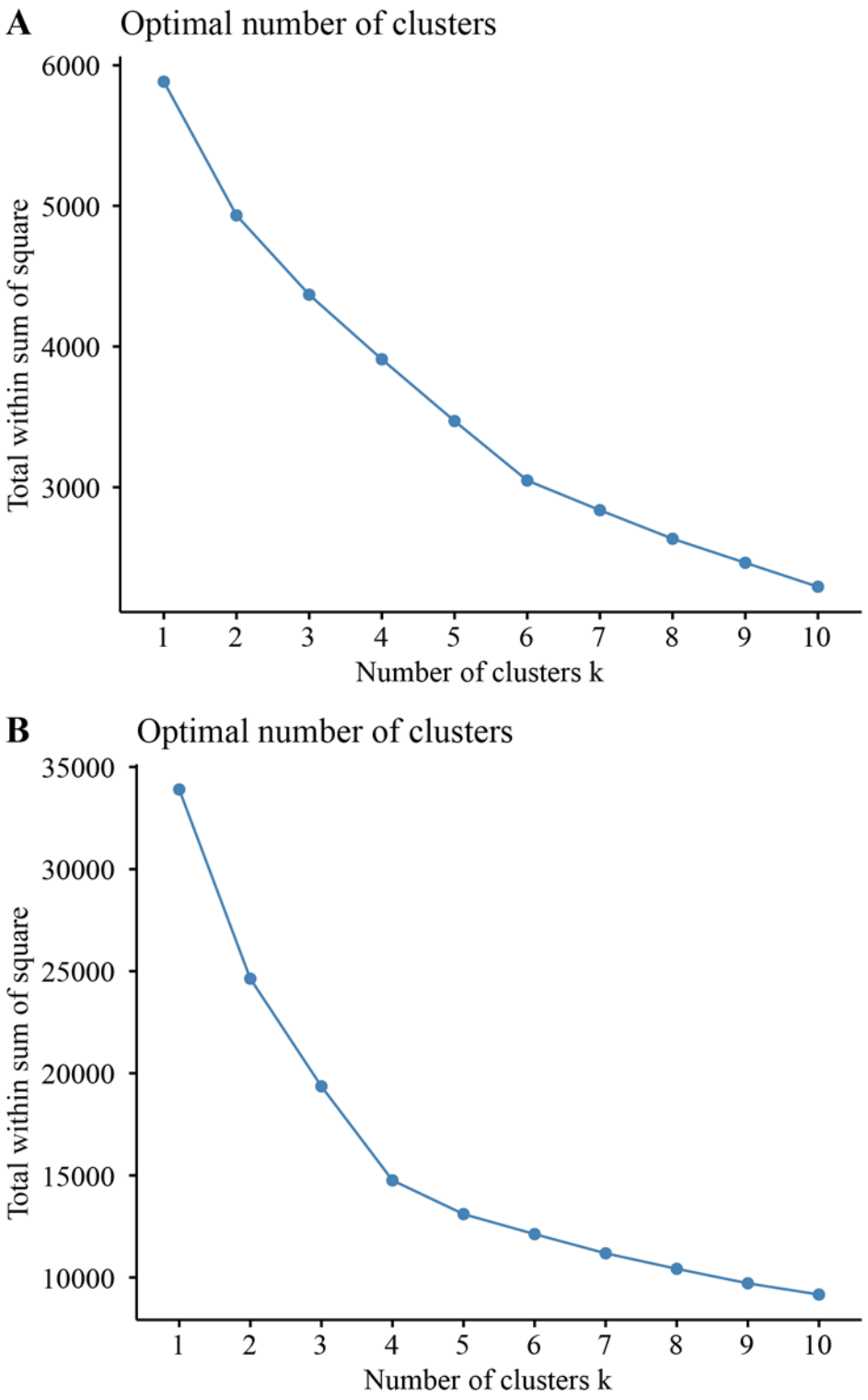

Figure S2. Optimal clusters based on elbow methods in hierarchical clustering analysis of differentially abundant ASVs at 2-h (A) and 4-h (B) EBCT.

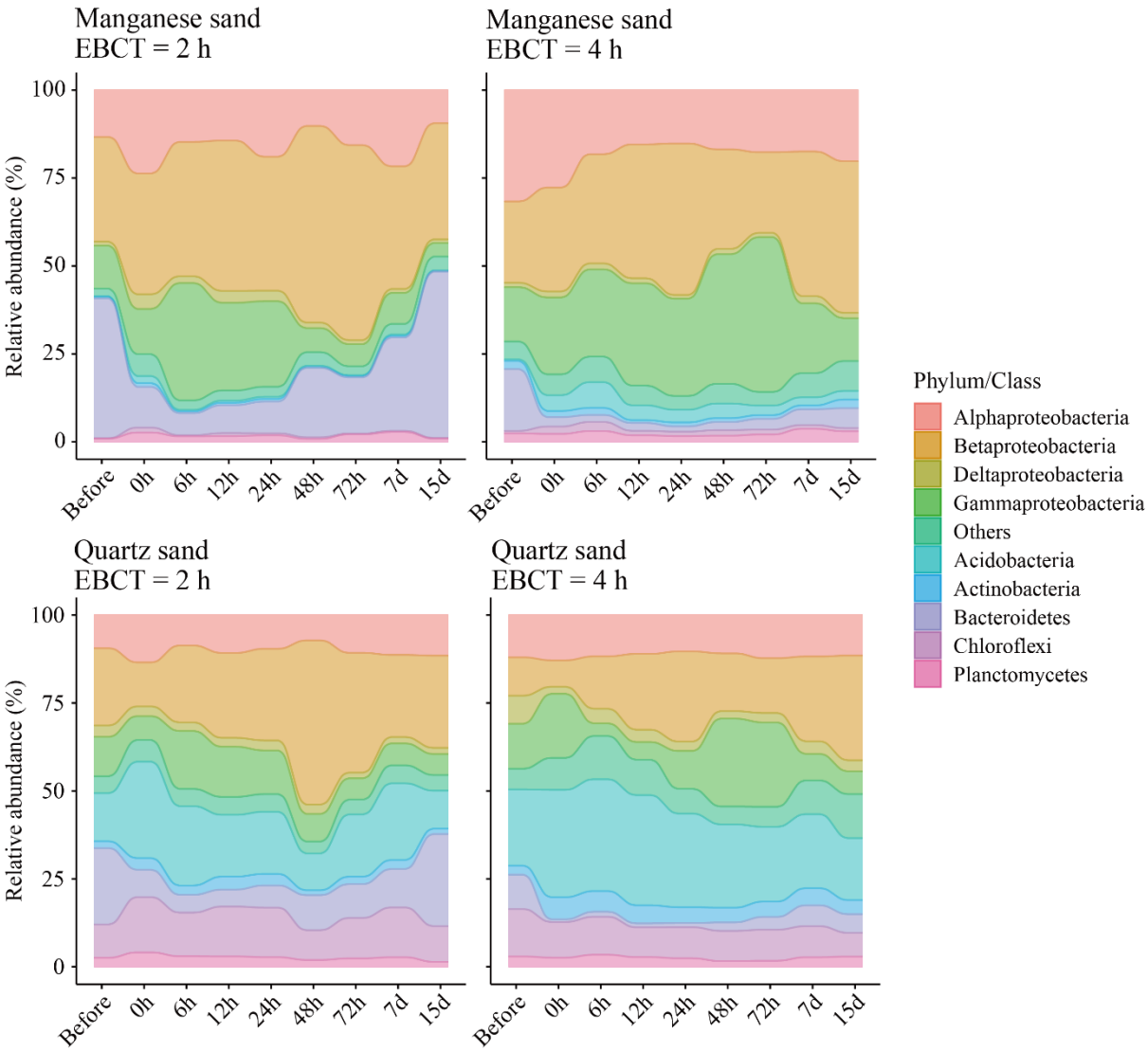

Figure S3. Changes in relative abundance of bacterial phyla before backwashing and at each time point after backwashing in two types of sand filters at three EBCTs. Proteobacteria were further classified into class level: Alpha-, Beta-, Delta-, and Gamma-proteobacteria. Others represent total relative abundance of all other phyla.

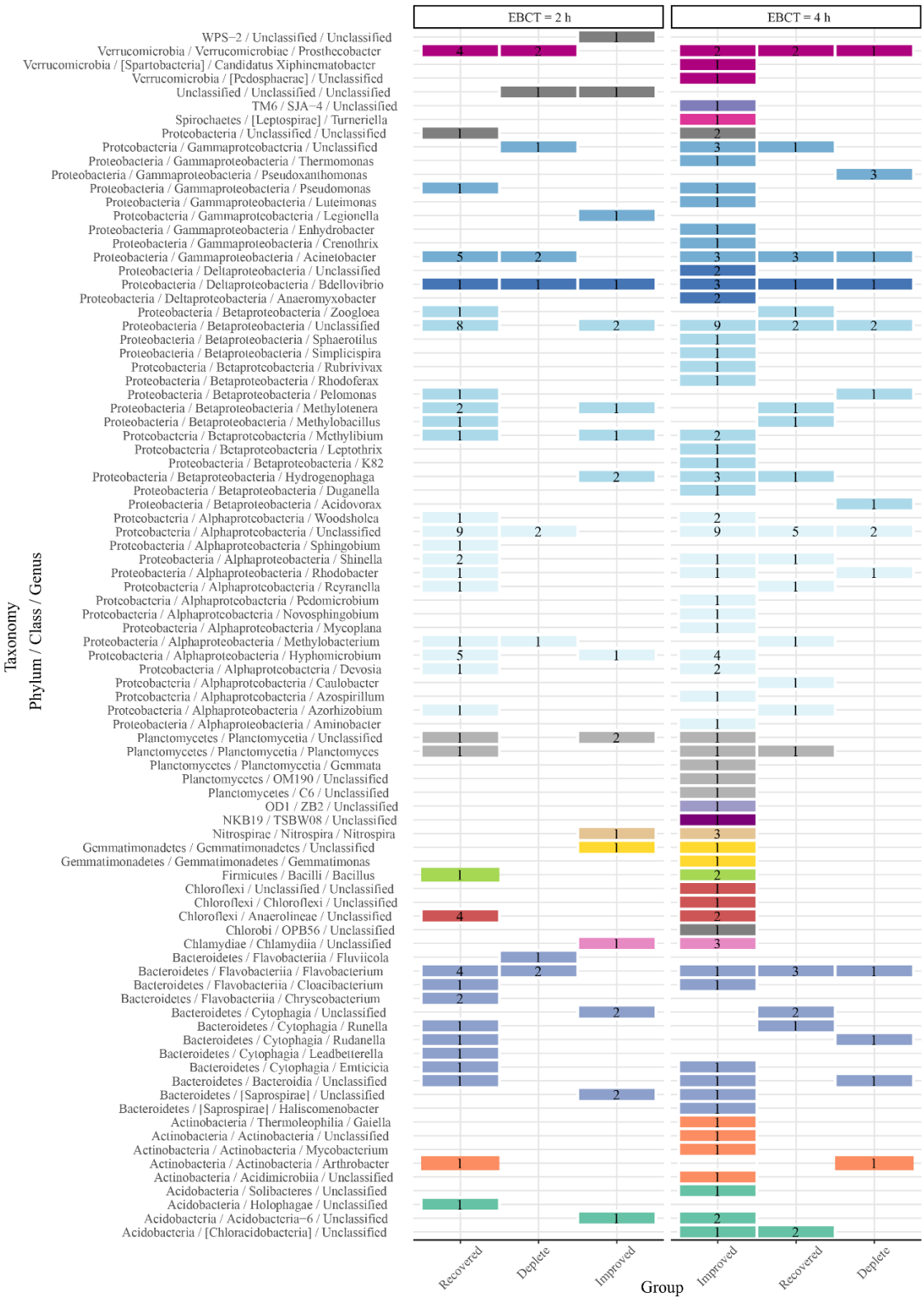

Figure S4. Modules of differentially abundant ASVs in manganese and quartz sand filters. Classification of differentially abundant ASVs in each distinct group detected through hierarchical clustering. Each tile indicates number of classified ASVs in a particular group. Settings of color are the same as in Figure 3.

References

Bolyen E, Rideout J R, Dillon M R, Bokulich N A, Abnet C C, Al-Ghalith G A, Alexander H, Alm E J, Arumugam M, Asnicar F, Bai Y, Bisanz J E, Bittinger K, Brejnrod A, Brislawn C J, Brown C T, Callahan B J, Caraballo-Rodriguez A M, Chase J, Cope E K, Da Silva R, Diener C, Dorrestein P C, Douglas G M, Durall D M, Duvallet C, Edwardson C F, Ernst M, Estaki M, Fouquier J, Gauglitz J M, Gibbons S M, Gibson D L, Gonzalez A, Gorlick K, Guo J, Hillmann B, Holmes S, Holste H, Huttenhower C, Huttley G A, Janssen S, Jarmusch A K, Jiang L, Kaehler B D, Bin Kang K, Keefe C R, Keim P, Kelley S T, Knights D, Koester I, Kosciolek T, Kreps J, Langille M G I, Lee J, Ley R, Liu Y-X, Loftfield E, Lozupone C, Maher M, Marotz C, Martin B D, Mcdonald D, Mciver L J, Melnik A V, Metcalf J L, Morgan S C, Morton J T, Naimey A T, Navas-Molina J A, Nothias L F, Orchanian S B, Pearson T, Peoples S L, Petras D, Preuss M L, Pruesse E, Rasmussen L B, Rivers A, Robeson M S, Ii, Rosenthal P, Segata N, Shaffer M, Shiffer A, Sinha R, Song S J, Spear J R, Swafford A D, Thompson L R, Torres P J, Trinh P, Tripathi A, Turnbaugh P J, Ul-Hasan S, Van Der Hooft J J J, Vargas F, Vazquez-Baeza Y, Vogtmann E, Von Hippel M, Walters W, Walters W, Wan Y, Wang M, Warren J, Weber K C, Williamson C H D, Willis A D, Xu Z Z, Zaneveld J R, Zhang Y, Zhu Q, Knight R, Caporaso J G (2019). Reproducible, interactive, scalable and extensible microbiome data science using QIIME 2 (vol 37, pg 852, 2019). Nature Biotechnology, 37(9): 1091-1091